PHYSICAL REVIEW B VOLUME 47, NUMBER 1 1 JANUARY 1993-I

Heat capacity and the commensurate-incommensurate transition of ^{4}He adsorbed on graphite

Dennis S. Greywall
AT&T Bell Laboratories, Murray Hill, New Jersey 07974
(Received 29 April 1992)

The heat capacity of ^{4}He adsorbed on graphite has been precisely measured over a fine grid of coverages for temperatures extending down to 100 mK and for coverages up to five atomic layers. This paper focuses mainly on the transitional region between the $\sqrt{3}\times\sqrt{3}$ commensurate structure and the incommensurate phase of the first adsorbed layer. At the commensurate coverage, $\rho_{1/3}$, the low-temperature data have been used to extract a phonon energy gap of 10.5 K, in agreement with the neutron-scattering value obtained for adsorbed ^{3}He. At coverages slightly greater than $\rho_{1/3}$ the data are consistent with an incommensurate domain-wall solid. However, an abrupt change in behavior occurs at $\rho=1.1\ \rho_{1/3}$, which is interpreted as signalling the entrance into a coexistence region involving a commensurate structure in which $\frac{2}{5}$ of the graphite adsorption sites are occupied by ^{4}He atoms. At $\rho_{2/5}$ the system undergoes a sharp first-order transition near 1 K where the entropy per atom changes by $0.2k_B$. At somewhat higher coverages there is evidence for a $\frac{3}{7}$ commensurate structure that transforms at 0.6 K into the floating incommensurate solid. Data for the second adsorbed layer indicate a solid registered relative to the compressed incommensurate first layer. Here the ratio of second- to first-layer densities is $\frac{4}{7}$, in agreement with recent results for ^{3}He on graphite.

I. INTRODUCTION

One especially interesting issue in the study of physisorbed monolayers concerns the competition between adatom-adatom and adatom-substrate interactions. This competition determines the detailed manner in which the two-dimensional (2D) system transforms between commensurate (C) and incommensurate (IC) solid structures.[1] The exact evolution therefore depends on the particular combination of adsorbate and substrate and can vary greatly while remaining consistent with modern theory which describes the C-IC transition in terms of the formation of various types and patterns of dense or rarified domain walls which separate commensurate regions. These domain walls can be highly mobile[2] at zero temperature and form a domain-wall fluid (DWF), or they can be fixed in a lattice which melts at finite temperature into the DWF. At sufficiently high temperature the DWF evolves into the isotropic 2D fluid phase.

For the case of krypton on graphite[3] the weakly incommensurate phase is a DWF which may exist down to $T=0$, followed at higher coverages by a hexagonal domain-wall solid and then the IC phase. Because of the small lateral contribution from the substrate potential, the IC phase has rotational epitaxy[4] with respect to the substrate lattice. For this system, the C-IC transitional region in very narrow and is restricted to within a few percent of the $\sqrt{3}\times\sqrt{3}$ commensurate coverage ($\rho_{1/3}=0.0637$ atoms/Å^2).

For H_2 adsorbed on graphite the quantum-mechanical effects associated with the small mass of these spherical molecules are important and here the transitional region[5] is very much larger with the IC phase being pushed to $\rho\gtrsim 1.2\ \rho_{1/3}$. This system is also different from krypton/graphite in that with increasing density the low-temperature system enters directly into a superheavy[6] striped domain-wall solid,[7] without passing through a reentrant fluid phase. The same is true for D_2/graphite[8,9] except here the striped phase gives way to a hexagonal heavy domain-wall structure before entering into the IC phase.

Because of the smaller polarizability of the helium atom, quantum effects should be significantly more important for this adsorbate, relative to hydrogen. This is immediately apparent from the fact that corresponding boundaries in the ρ-T phase diagram occur at temperatures an order of magnitude smaller. But aside from this temperature rescaling, the qualitative features of the phase diagrams for hydrogen and helium appear remarkably similar. This has prompted some to speculate that, at least near the C-IC transition region, there may be a generic phase diagram for the quantum adsorbates. This supposition is necessary because even though the large transitional region was first observed for helium,[10] the helium systems have not yet been explored in detail. This is presumably due to the lower temperatures involved, the low neutron-scattering cross section, and the problems associated with the background reflection from graphite. However, given the significant differences between the H_2 and D_2 results, one should be extremely cautious about assuming analogous behavior for the helium isotopes. Evidence that something unusual may be occurring for adsorbed helium comes from the low-millikelvin temperature heat capacity of ^{3}He/graphite. These data show, as a function of coverage, an intriguing peak in the nuclear-spin contribution[11,12] which can be understood only if more is known about the structural behavior of the 2D solid in this transitional regime.

In this paper we present a detailed set of heat-capacity results for the solid phases of ^{4}He/graphite. Although

 ©1993 The American Physical Society

some results for the solid phases of the second adsorbed layer are discussed, the main emphasis is on the C-IC transitional region of the first layer. The measurements were made at a number of closely spaced coverages and extend to lower temperatures than in previous experiments. The precision of the data permitted an accurate determination of the temperature dependence for each sample down to about 100 mK. Near the $\frac{1}{3}$ coverage a defect contribution was observed, but it was still possible to determine the energy gap in the phonon-dispersion relation. In contrast to the findings for other adsorbates on graphite, it is claimed that the intermediate region between the $\frac{1}{3}$ and the IC phases is dominated by a higher-order registered phase. The entropy change on melting into the DWF has been determined. At somewhat higher coverages a new solid phase was observed which transforms directly into the IC phase on warming. Evidence is also presented which suggests that the second layer freezes into a solid which is registered with respect to the first layer.

II. EXPERIMENTAL DETAILS

A cross-sectional drawing of the calorimeter is shown in Fig. 1. The substrate assembly consists of 78 elements separated by silver washers and tightly clamped to the base of the cell with a silver bolt. Each element is a disk of thin silver foil with annular disks of 0.13-mm-thick grade GTA Grafoil[13] bonded[12] to either side. This assembly is covered with a thin silver shell and rigidly supported on three Vespel[14] tubes. These tubes, along with a fine copper wire, provide the weak thermal contact to the support platform which in turn is joined to the mixing chamber of a dilution refrigeration via a superconducting tin heat switch. Various heaters and thermometers are mounted on a flange attached to the cell base. These include a calibrated germanium thermometer, a 470-Ω Speer thermometer, a 10-kΩ reference resistor, the main heater (435 Ω), and an auxiliary (10-kΩ) heater.

The masses of silver and graphite in the calorimeter are 125 and 14.2 gms, respectively. The dead volume is 18 cm^3, and the total surface area is 261 m^2. This surface area calibration is based on the assumption that the largest order-disorder heat-capacity peak occurs at the completion of the perfect $\frac{1}{3}$ commensurate structure. The cell was evacuated at room temperature using a small copper tube which was then crimped closed.

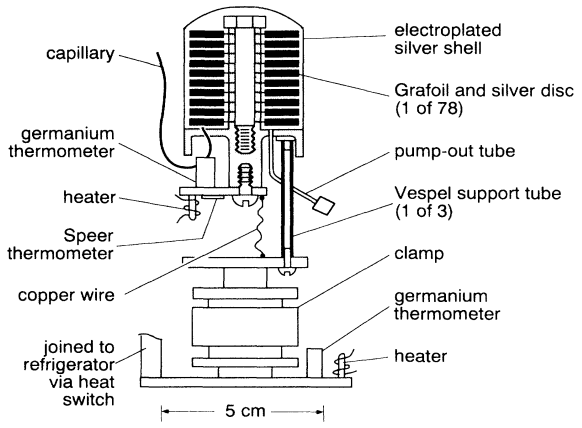

FIG. 1. Calorimeter.

The sample coverages were generated by making precisely measured incremental additions to the amount of high-purity ^4He (2.4 ppb ^3He) in the calorimeter. These samples were annealed at an elevated temperature (15 K for the lowest coverage samples) for several hours and then cooled over a period of 12–18 h to the starting temperature of 90 mK. The cooling was carefully monitored to determine the temperature location of any heat-capacity anomalies so that these regions later could be given special attention.

The heat-capacity data were then taken on warming, using the usual heat-pulse technique. Prior to the application of each pulse a warming drift rate was generated by raising and regulating the temperature of the supporting platform. After the pulse (typically 20 s in duration) the cell cooled from the higher temperature at a similar rate. Thermal relaxation times were on the order of seconds. Near 0.7 K it became more difficult to change and regular the support platform temperature and so it was left fixed at this level. The drift rate was then adjusted using the auxiliary heater on the cell flange.

All of the data were corrected for the addendum contribution to the total heat capacity. This contribution was smooth and could be accurately described by a simple fitting function. Above monolayer completion a correction was also applied for desorption effects.

III. RESULTS AND DISCUSSION

A. Heat-capacity data

The heat-capacity results for the 84 samples studied are shown plotted as a function of temperature in Figs. 2 and 3. The solid curves were computer drawn and are spline fits passing through each of the data points or are, in the case of sharp peaks, simple point-to-point connections. The total coverage expressed in units of atoms/$Å^2$ is indicated in each of the component figures. Figure 2 shows the first-layer results. Figure 3 shows results for the second, third, fourth, and fifth layers, where layer promotions occur at 0.120, 0.212, 0.288, 0.364, and 0.440 atoms/$Å^2$, respectively.[15] The data of Fig. 3 have been corrected for desorption and for the small contribution from the compressed first layer.

The overall interpretation of the first-layer data is summarized by the phase diagram shown in Fig. 4, where G, L, and F refer to gas, liquid, and fluid. The lower coverage portion of the diagram was discussed in a previous publication,[15] where it was proposed that the system undergoes a gas-liquid phase separation near 1 K. The main emphasis here is on the higher coverage data and in particular on the transitional regime separating the C and IC phases. Figure 2 shows that this region ($0.064 \lesssim \rho \lesssim 0.080$) is dominated by the presence of an extremely sharp heat-capacity peak near 1 K.

To more concisely show the effects due to changes in areal density, the first-layer results are plotted along

several isotherms in Figs. 5(a)–5(e). The upper two panels in this figure, 5(f) and 5(g), show, respectively, the amplitude and the temperature location of the various heat-capacity peaks which were used in part to determine the phase diagram of Fig. 4. Several special coverages are indicated by vertical dashed lines which are labeled A through D and correspond to densities of 0.0637, 0.0663, 0.0760, and 0.1200 atoms/Å^2, respectively. ρ_A ($\equiv\rho_{1/3}$) is the coverage of the largest commensurate phase heat-capacity peak which by convention is taken to be that corresponding to the perfect commensurate structure with precisely one-third of the graphite adsorption sites occupied by helium atoms. It should be noted, however, that there is an ambiguity in this coverage scale of several percent as discussed below and as observed previously in neutron-scattering experiments.[16]

One would have expected each of the low-temperature heat-capacity isotherms to show a feature at perfect regis-

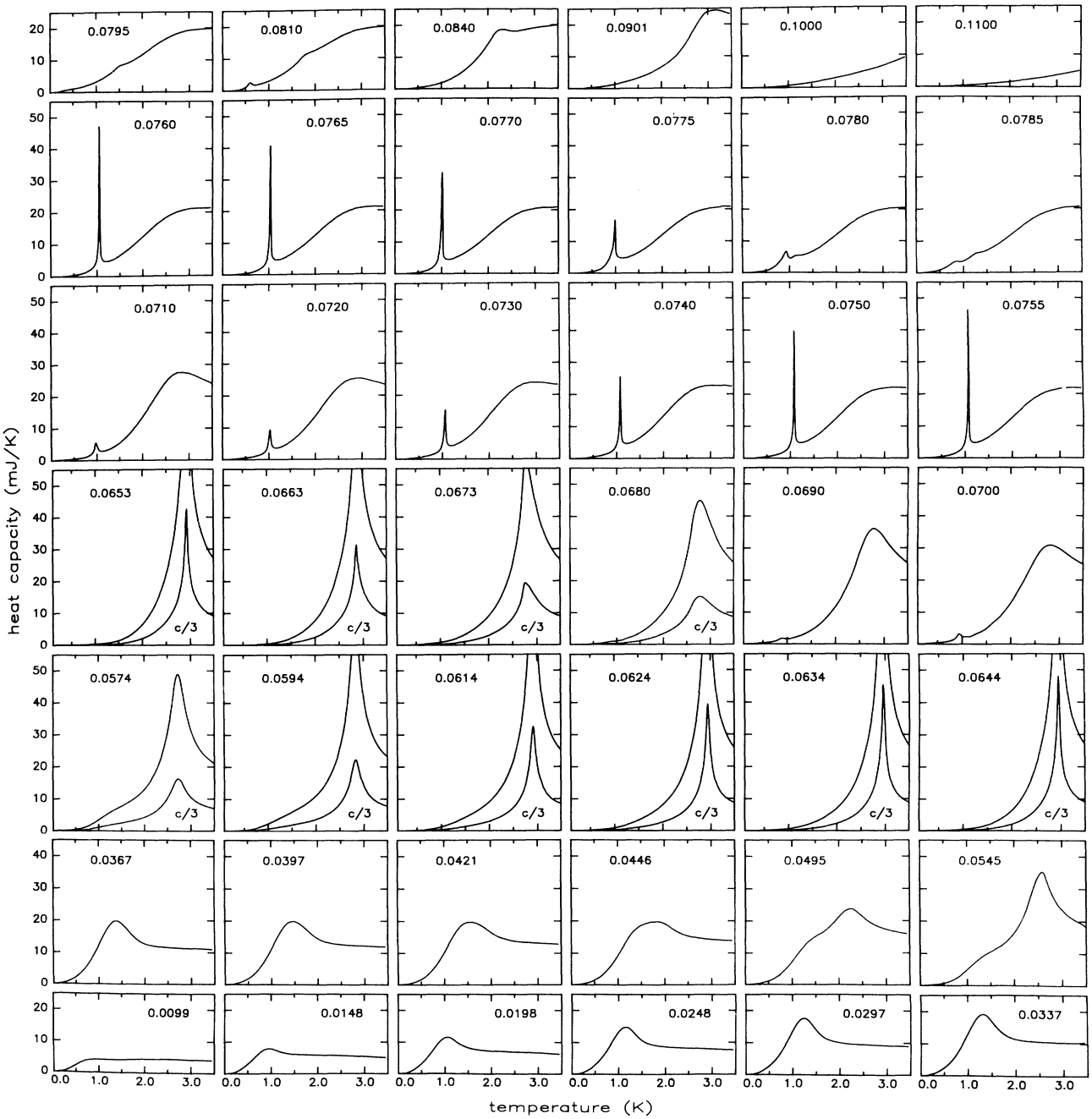

FIG. 2. Heat-capacity results for several submonolayer coverages given in atoms/Å^2. The solid curves were computer drawn and are spline fits passing through each of the data points or are, in the case of sharp peaks, simple point-to-point connections.

try. The data, however, exhibit a sharp minimum at ρ_B which is 4% larger than ρ_A. At ρ_B there is also a kink in the locus of order-disorder peak temperatures versus ρ [Fig. 5(g)] and also the first appearance of a new heat-capacity peak near 1 K. With increasing density, this peak grows rapidly into the large and very sharp anomaly first observed by Hering, Van Sciver, and Vilches.[10] It is associated with the C-IC transition and reaches its maximum amplitude at ρ_C. Promotion of atoms into the second layer occurs at ρ_D.

For coverages between 0.04 and ρ_A, the $\frac{1}{3}$ commensurate solid coexists with the 2D fluid phase.[15] As required by thermodynamics the low-temperature isotherms are linear functions of areal density over most of this coverage regime. The break in the low-temperature isotherms near 0.06 (which is also seen in the ^{3}He/graphite isotherms[11]) is presumably due either to the existence of zero-point vacancies or more probably to the finite size of the homogeneous regions on the graphite substrate. The finite size implies that several percent of the adsorbed

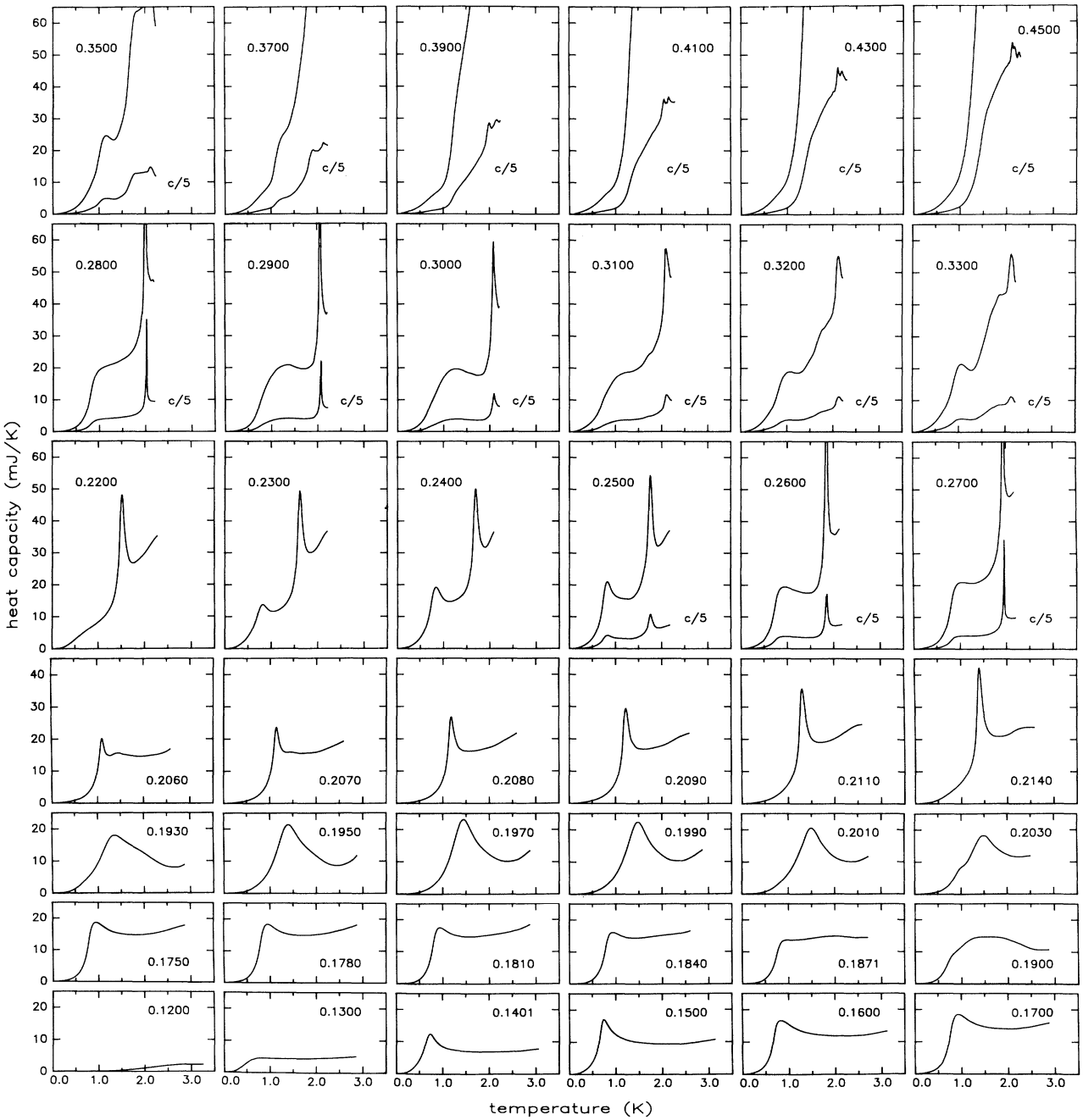

FIG. 3. Heat-capacity results obtained for the second through the fifth layers. These data have been corrected for desorption and for the small contribution from the compressed first layer. The numbers give the total coverage in atoms/A^2.

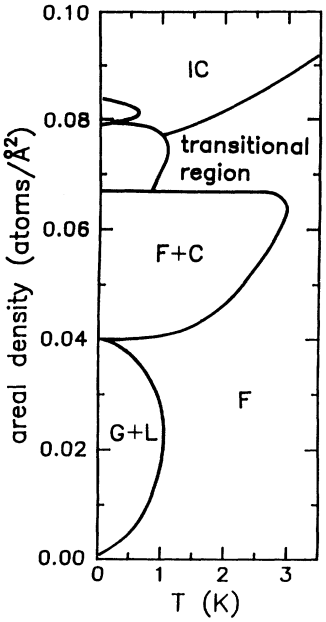

FIG. 4. Proposed phase diagram for ^{4}He adsorbed on graphite.

atoms lie along the perimeters of these regions and therefore experience a weaker attraction to the substrate and an altered in-plane interaction with the remainder of the helium atoms. Our belief is that for $0.06 \lesssim \rho \lesssim \rho_B$ changes are occurring primarily along the perimeter and that the destruction of the perfect commensurate structure in the interior of the homogeneous regions occurs only for $\rho > \rho_B$.

Extrapolations of the 0.1 and 0.2 K isotherms between 0.04 and 0.06 out toward higher coverages yield heat-capacity values at ρ_B much larger than actually measured at that coverage. This suggests that the very low-temperature heat capacity in this coverage regime is dominated by a large nonsolidlike contribution from the perimeter atoms. The measured rapid decrease toward zero heat capacity at ρ_B suggests that these perimeter atoms begin to localize near 0.06.

B. $\sqrt{3}\times\sqrt{3}$ commensurate solid

The lack of translational invariance for a commensurate solid leads to an energy gap Δ in the acoustic branch of the phonon-dispersion relation at the zone center. Consequently one should expect the low-temperature heat capacity of this solid to be extremely small and to be described by an expression of the form $T^{-2}e^{-\Delta/T}$. None of the data obtained near $\rho_{1/3}$, however, are accurately described by this simple expression, especially at the lowest temperatures where there is an extreme sensitivity to other contributions. Adding a constant term to the function improved the fits, but the best fits were obtained by also including a term in T^2. A fit to the expression

$$\frac{c}{Nk_B} = \alpha + \beta T^2 + \left[\frac{\gamma}{T}\right]^2 e^{-\Delta/T}$$

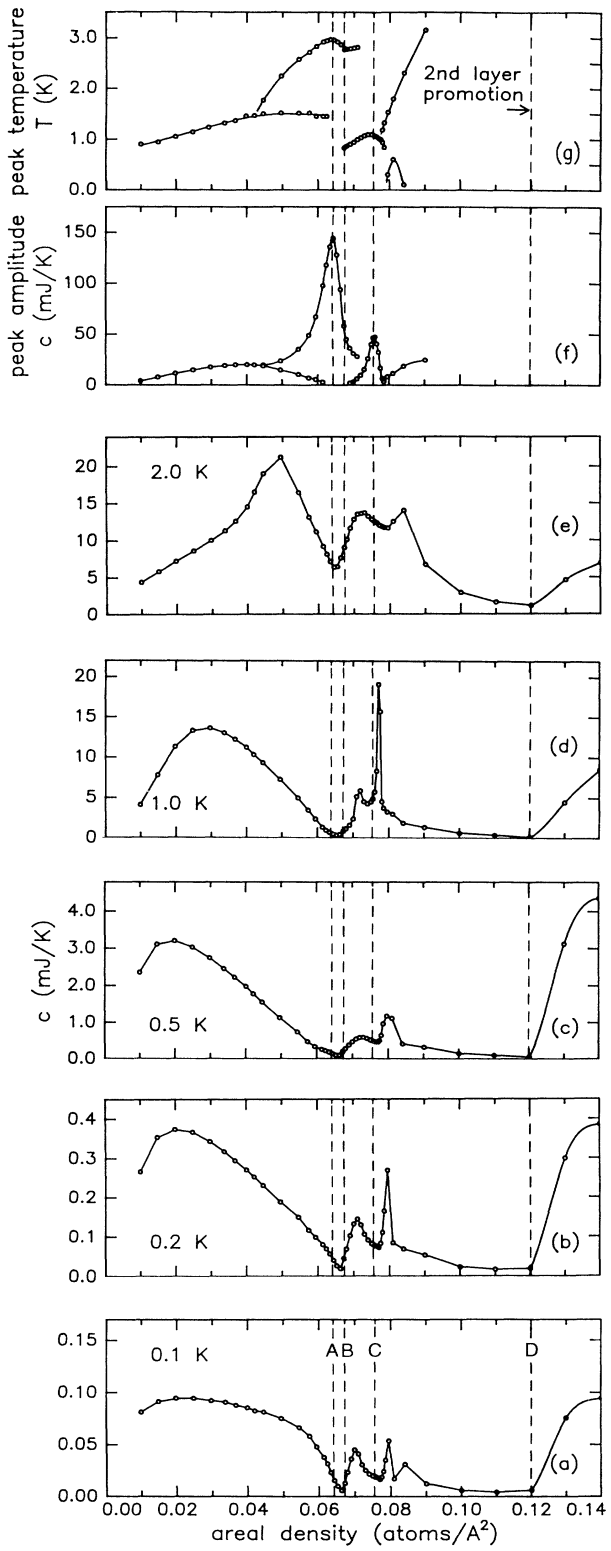

FIG. 5. First-layer heat capacity as a function of coverage for several isotherms. The upper two panels show the amplitude and the temperature location of various heat-capacity peaks. Special coverages, referred to in the text, are labeled *A*–*D*.

using the data obtained at $\rho_B=0.0663$ and for $0.3<T<1.5$ K yielded

$$\alpha=(6.3\pm0.4)\times10^{-4},$$

$$\beta=(1.45\pm0.01)\times10^{-2}\ \mathrm{K}^{-2},$$

$$\gamma=12\pm1\ \mathrm{K}$$

$$\Delta=10.5\pm0.1\ \mathrm{K},$$

with a rms deviation of 0.8%. Including data at lower temperatures leads to increasing systematic deviations, suggesting the need for a more complicated function and also reflecting the increasing relative uncertainty in the data.

The best-fit energy gap, namely 10.5 K, agrees with the ^{3}He value 10.9 K extracted from inelastic neutron-scattering measurements,[17,18] but differs from the theoretical[19] energy gap of 16 K.

Fits performed at slightly lower coverages gave similar results but with a general trend toward larger values of both α and β with decreasing ρ. At ρ_A, a fit with Δ held fixed at 10.5 K gave $\alpha=(19\pm2)\times10^{-4}$ and $\beta=(1.75\pm0.04)\times10^{-2}$. The first coefficient might be interpreted as indicating that 0.2% of the ^{4}He atoms make a classical contribution to the total heat capacity, while β suggests that roughly 3% of the atoms have a fluidlike heat capacity. This last estimate is based on a fluid specific heat of $0.56T^2$ determined at $\rho=0.0367$. As the density is increased to ρ_B it is mainly the classical contribution, perhaps due to vacancies, which decreases. At coverages greater than ρ_B, the quality of the fits worsened dramatically, coinciding with the emergence of a new peak at 1 K.

C. *C*-IC transition

The sharp 1-K peak associated with the density region directly above the commensurate solid is first discernible in log-log plots of the data at a coverage of 0.0673. Since this peak, which is presumably due to the melting of a domain-wall solid, appears immediately above ρ_B, the evidence is against the existence of a reentrant fluid phase extending to zero temperature. Although the 1-K peak first appears with a very small amplitude, Fig. 5(f) shows that it grows rapidly with coverage and reaches a maximum amplitude of $1.8Nk_B$ at $\rho=0.0760$.

Data obtained near this coverage are shown on an expanded temperature scale in Fig. 6. For clarity actual data points are plotted only for the coverage of the largest peak. The other curves are spline fits determined by a similar spacing of measured values. In agreement with the results of Hering, Van Sciver, and Vilches,[10] the largest peak (curve *f*) occurs at a coverage slightly higher than that of the highest transition temperature (curve *d*). It should also be noted that our maximum amplitude is 50% greater than the earlier result and has a width $\Delta T/T$ of about 2%. Figure 7 shows that this peak is much sharper that the 3 K peak corresponding to the order-disorder transition of the $\frac{1}{3}$ commensurate phase. For this latter transition the data[20] are described well by the relation $C\propto|t|^{-\alpha}$, where t is the reduced temperature

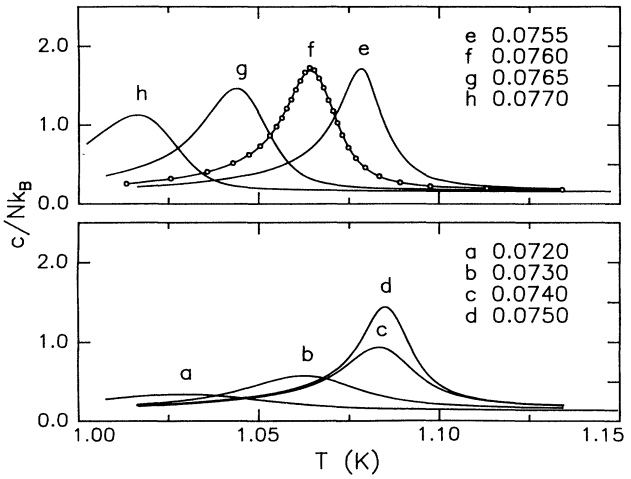

FIG. 6. Heat capacity plotted on an expanded temperature scale for coverages near 0.0760 atoms/A^2. The solid curves are spline fits of the data.

$|T-T_c|/T_c$ and α is consistent with $\frac{1}{3}$ both above and below the transition in agreement with the three-state Potts model.[21] Fits of the data at $\rho=0.0760$ using this same expression showed significant systematic deviations, but over an order of magnitude in t yielded an exponent of unity, implying immediately that this transition cannot be continuous.

In general, warming through a first-order transition at constant density should yield a heat capacity which ideally shows a discontinuous increase as the system enters the two-phase region (due to the latent heat), followed by a discontinuous decrease at a higher temperature as the system enters again into a pure-phase-region state. The absence of a well-defined two-phase region in the data near 0.076 implies an extremely small difference in density between the low- and high-temperature phases. In fact this difference should be precisely zero based on a Clausius-Clapeyron relation, since the phase boundary mapped out by the heat-capacity peaks (Fig. 4) is locally independent of coverage. The heat-capacity feature should therefore be a δ function. The finite peak width

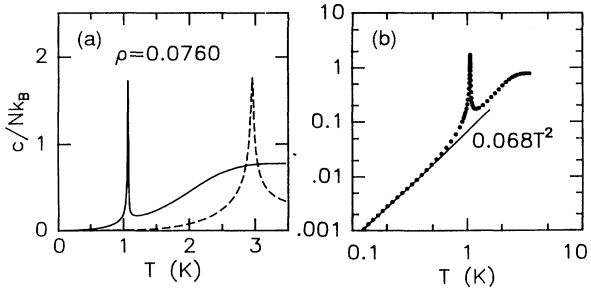

FIG. 7. (a) Comparison of the sharp heat-capacity peak measured in the transitional region ($\rho=0.0760$) and the order-disorder peak of the commensurate phase, dashed curve ($\rho=0.0644$). The *C*-phase peak has been reduced by a factor of 3. (b) Log-log plot of the data at $\rho=0.0760$ showing the T^2 temperature dependence at low temperatures.

indicates small areal density variations within the sample.

The heat capacity corrected for the latent heat contribution is shown as a dashed curve in Fig. 8. This curve was obtained by simply extrapolating the T^2 behavior determined both below and above the transition in toward the peak temperature [see Fig. 7(b)]. The solid curve shows the entropy obtained by integrating this extrapolated heat capacity divided by the temperature. The large jump in the entropy at the transition of about $0.2k_B$ per atom is the integral of the difference between the measured and extrapolated heat capacities.

The locus of peak temperatures versus the coverage, Fig. 5(g) is smooth over the range $\rho_B < \rho < 0.08$ with no obvious features to suggest that this region of the phase diagram consists of more than a single phase. On the other hand, the low-temperature isotherms, Figs. 5(a) and 5(b), do suggest two regions with a boundary near 0.07.

Between ρ_B and 0.07 the low-temperature isotherms grow linearly with coverage. A theoretical calculation by Halpin-Healey and Kardar[22] indicates that at coverages immediately above $\rho_{1/3}$ the commensurate phase should give way to a domain-wall fluid extending to zero temperature. If this were the case the heat-capacity peak at 1 K might be associated with a transition into the isotropic fluid phase. The problem with this interpretation is that the 1-K peak continues to exist at coverages well above ρ_B where the theory indicates a striped incommensurate solid phase. Moreover there is a rounded maximum near 3 K which evolves from the order-disorder peak of the $\frac{1}{3}$ phase and which is more likely signalling the transformation into the isotropic fluid state. Prejudiced by the theoretical prediction for the slightly higher coverage regime and also by what is known from neutron-scattering measurements about the H_2/graphite system, we speculate that the weakly incommensurate phase for helium is a striped phase with superheavy domain walls, perhaps with an extremely narrow intervening fluid phase. It should be noted though that the regime $\rho_\beta < \rho < 0.07$ could also correspond to a coexistence between two commensurate phases.

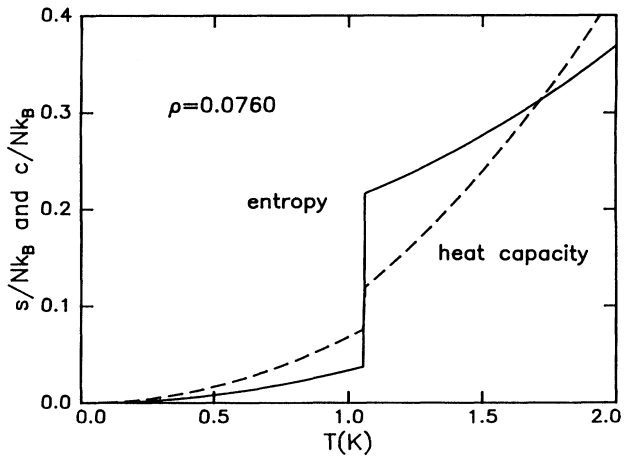

FIG. 8. Smoothed results for the entropy and the specific heat of the $\frac{2}{5}$ phase.

The low-temperature isotherms exhibit a dramatic change in behavior at 0.07; here the heat capacity at fixed temperature suddenly starts to decrease. Assuming the striped-phase picture, this occurs when there are about eight commensurate rows per domain and most likely signals the point at which the increasing wall interactions lead to an unstable configuration. This could possibly be resolved by the system forming a different type of wall and/or changing the wall arrangement from striped to hexagonal. Another possibility to consider, however, is that at 0.07 the system enters into a coexistence region in which one of the phases is a (presumably striped) *commensurate* phase with a density near 0.076. This would imply that $\frac{2}{5}$ of the graphite absorption sites are occupied by helium atoms. The suggestion of a $\frac{2}{5}$ commensurate phase is advanced for several reasons. (1) The sharp maximum in peak amplitude versus coverage [Fig. 5(f)] singles out $\rho = 0.076$ as a special coverage. (2) The amplitude of the 1-K peak evolves as a function of coverage in a manner very similar to that of the $\frac{1}{3}$ phase [Fig. 5(f)]. (3) The low-temperature heat capacity is smallest when the 1-K peak has its greatest amplitude, again in agreement with the behavior near $\rho_{1/3}$. (4) At a coverage a few percent less than 0.076 the low-temperature isotherms show a break in behavior similar to that observed for the $\frac{1}{3}$ phase. [Compare Fig. 5(a) at $\rho \lesssim 0.076$ with Fig. 5(c) at $\rho \lesssim 0.064$. In Sec. III A, this break was interpreted as indicating that helium atoms along the perimeter of homogeneous regions on the substrate are more difficult to localize.] (5) Nuclear-spin heat-capacity isotherms for ^{3}He/graphite show a sharp maximum at 0.076. This suggests a special arrangement of atoms which enhances atomic exchange. Of course, the assumption is that absorbed ^{3}He and ^{4}He behave in a similar manner in this region of the ρ-T phase diagram.

Figure 9(a) shows one possible atomic arrangement for the $\frac{2}{5}$ phase in the lattice-gas limit in which the atoms are centered in absorption sites. It is a striped structure with heavy domain walls and a structure which suggests the possibility of unusual exchange for ^{3}He.

Although the order-disorder transition for the $\frac{1}{3}$ phase is continuous, the transition for the $\frac{2}{5}$ phase, as discussed above, is first order. This is not surprising since the order-disorder transition is expected[23] to be continuous for relatively few commensurate structures. What is surprising is that the low-temperature heat capacity, Fig. 7(b), shows a temperature dependence which is clearly not of the activation type but instead T^2. This suggests either a very small energy gap in the phonon-dispersion relation or a sizable contribution to the heat capacity from the atoms along the perimeter of the homogeneous regions on the graphite substrate. See Sec. III B.

For the case of H_2/graphite the entire C-IC transitional region is associated with a single (α) phase. The hydrogen heat-capacity peaks in this region are not nearly as sharp as the helium peaks and reach a maximum amplitude[5] of only $0.5Nk_B$ at 9 K and at $\rho = 0.072$. The temperature dependence below the peak was not reported. At a coverage of 0.075 the α phase is replaced by the IC solid phase.

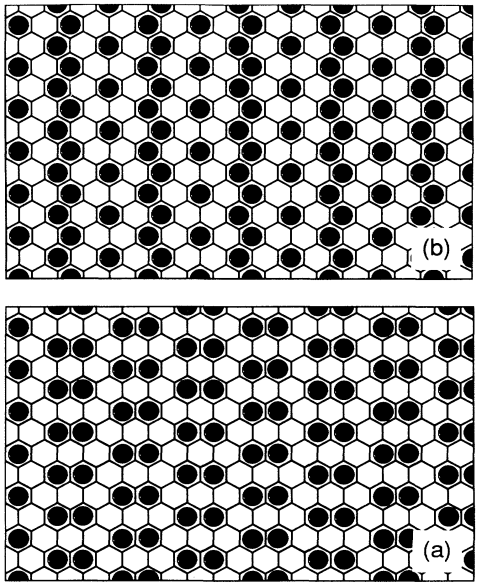

FIG. 9. Possible commensurate structures for ^{4}He/graphite in the lattice-gas limit. (a) A structure in which $\frac{2}{5}$ of the adsorption sites are occupied by ^{4}He atoms, $\rho=0.0764$ atoms/Å^2. (b) A structure in which $\frac{3}{7}$ of the adsorption sites are occupied by ^{4}He atoms, $\rho=0.0818$ atoms/Å^2.

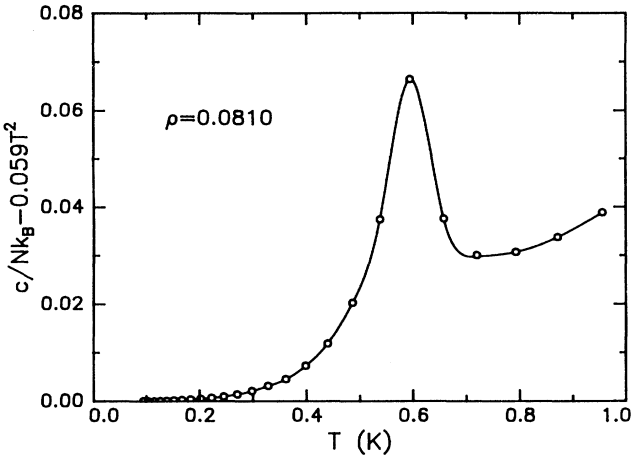

FIG. 10. Specific heat of the $\frac{3}{7}$ commensurate phase of ^{4}He/graphite. A T^2 background contribution has been subtracted.

Deuterium on graphite exhibits a wider intermediate region which is considerably more complicated than the corresponding region for hydrogen. In particular, near $\rho=0.075$ the α phase transforms via a first-order transition into the γ phase which then yields to other phases (δ,ε) at low temperatures and finally to the floating IC phase at a coverage of 0.086. The γ phase is found[9] to be consistent with a hexagonal incommensurate solid phase with heavy domain walls.

D. $\frac{3}{7}$ phase

Coinciding with the near extinction of the sharp 1-K peak at a coverage of 0.078 is the emergence of a very rounded peak at a higher temperature (see Fig. 2). This peak moves rapidly up in temperature with increasing coverage and corresponds to the melting of the IC solid into the DWF phase, Fig. 4. However, for a narrow range of coverages slightly above 0.078 a second peak is also observed but now at a much lower temperature. The highest transition temperature for this new phase is 0.6 K and is reached at a coverage of 0.0810. Figure 10 shows this peak plotted relative to a large T^2 background contribution.

This phase is referred to as a $\frac{3}{7}$ phase since 0.081 is very close to the coverage (0.082) of a commensurate phase in which $\frac{3}{7}$ of the graphite adsorption sites are occupied by helium atoms. One possible striped structure is shown in Fig. 9(b). Another possibility is that this phase is equivalent to the δ phase of D_2/graphite which has been taken to be a higher-order commensurate $5\sqrt{3}\times5\sqrt{3}$ structure in which $\frac{31}{75}$ of the lattice sites are occupied by atoms. Here $\rho=0.079$. In the deuterium work,[9] it was found that this higher-order commensurate structure arises because of a special rotational behavior of the γ phases within which the δ phase appears. For ^{4}He/graphite there is no γ phase and so this argument does not apply.

E. Second-layer commensurate solid

At a coverage of 0.120 atoms/Å^2, atoms are promoted into the second layer. This is indicated in Fig. 5 by the rapid increase in all of the isotherms at $\rho=\rho_D$. The second layer then follows an evolution[15] quite similar to that of the first layer: at the lowest second-layer coverages there is a coexistence of 2D gas and liquid, at somewhat higher densities a coexistence of fluid and commensurate solid, and at the highest coverages a pure incommensurate solid phase.

The G-L region is identified by a rounded peak in the heat capacity near 0.7 K, Fig. 3. Near $\rho=0.19$ the peak associated with the commensurate phase emerges at 1.5 K and with a further small increase in coverage develops into the sole feature with the largest amplitude at a total coverage of 0.197 and at a second-layer density of 0.070 atoms/Å^2. The latter value assumes an estimated compressed first-layer density of 0.127, which is based on our determination of the density at layer promotion and on the subsequent relative compression inferred from measured shifts[24] in the melting temperature of the first-layer incommensurate solid. The identification of this peak as being due to the melting of a commensurate phase is based mainly on analogy with the first-layer phase diagram. In addition, however, we find that the 1.5 K peaks show little density dependence and exist over only a very restricted range of second-layer density as would be expected for a registered structure. Registry here, however, must be with respect to the first incommensurate solid layer of ^{4}He since the corrugation in the potential due to the graphite substrate is insignificant at the level of the second ^{4}He layer. This is exactly the

same reasoning and conclusion reached for the second layer of ^{3}He adsorbed on graphite. In that work, however, there was some ambiguity about the importance of the role of the graphite since the density of the second-layer registered phase for ^{3}He was estimated to be 0.064, which is very close to that required for $\sqrt{3}$ registry with respect to the graphite. The higher second-layer density for ^{4}He is a consequence of the tighter binding of ^{4}He to the substrate and the corresponding higher density of the compressed first layer. The ratio of the density of the second registered layer to that of the compressed underlying first layer is $0.55 \approx \frac{4}{7}$, in excellent agreement with the findings for ^{3}He/graphite, suggesting the same registered structure for both isotopes. Elser[25] has proposed that this structure is a $\sqrt{7} \times \sqrt{7}$ triangular lattice structure with one-quarter of the second-layer atoms located directly above the first-layer atoms and therefore at potential energy maxima. This structure not only possesses the experimental density, relative to the first layer, but can be used for the case of ^{3}He to explain the unusual nuclear magnetic properties of this solid phase.

The melting of the second-layer commensurate phase takes place over an extended temperature range with a rather rounded heat-capacity peak; see Fig. 3 at $\rho = 0.197$. This suggests that the transition is second order or possibly weakly first order with large precursors to the transition. For the triangular substrate provided by the first adsorbed layer, the order-disorder transitions that are predicted to be continuous belong to the universality classes of the Ising, the three-state Potts, and the four-state Potts models.[22] The 2D Ising model gives a logarithmic divergence of the heat capacity at T_c, while the Potts models lead to power-law divergences of $\frac{1}{3}$ and $\frac{2}{3}$, respectively. In principle it should be easy to distinguish between these very different types of critical behavior. In the present case, however, the rounding is extreme, possibly due to stresses induced in the first solidified layer of ^{4}He by the periodicity of the graphite holding potential. Because the amplitude of the measured heat-capacity peak is not large, the analysis of the data is overly sensitive to the nonsingular contribution to the heat capacity. There are also uncertainties due to the significant desorption corrections. Given these difficulties, we nonetheless tried fitting the data and found a marginal preference for a logarithm divergence. This would seem to provide some evidence against the proposed $\sqrt{7} \times \sqrt{7}$ structure which should undergo a first-order transition. It is possible, however, that an Ising-like symmetry could be introduced if the chirality of the structure plays a dominant role.[26]

As the areal density is increased from 0.197 to 0.203, the melting peak of the second-layer commensurate phase remains near 1.5 K. But at higher densities this feature is replaced by a sharper peak which first appears at 1 K and then moves toward higher temperatures. The significant density dependence of the temperature location of this peak prior to third-layer promotion suggests that it corresponds to the melting of the second-layer IC solid phase. There is no indication of an intermediate phase. Instead it appears that there is a simple two-phase coexistence region separating C and IC second-layer phases.

Note that since promotion into the third layer occurs[15] at $\rho = 0.212$, the second layer completes its evolution into the IC phase before a significant number of atoms occupy the next level. This is quite different from the ^{3}He/graphite systems where low-mK heat-capacity isotherms clearly show that atoms are promoted into the third level immediately following the formation of the second-layer registered phase.

The low-temperature isotherms at higher coverages [see Fig. 2(a) of Ref. 15] suggest that the third layer may also solidify into a registered structure prior to promotion into the fourth level. The absence of melting peaks to verify this could be explained by desorption depleting the third layer at the higher temperatures. This would not be true at much higher coverages, but then the heat capacity is dominated by the fluid layers which exhibit a precursor to the λ peak of bulk ^{4}He.

ACKNOWLEDGMENTS

I am grateful to M. H. W. Chan, S. N. Coppersmith, V. Elser, D. A. Huse, and O. E. Vilches for many valuable discussions. I also acknowledge the expert technical assistance of Paul A. Busch.

[1]See, e.g., M. den Nijs, in *Phase Transitions and Critical Phenomena,* edited by C. Domb and J. L. Lebowitz (Academic, New York, 1988), Vol. 12, p. 219.

[2]S. N. Coppersmith, D. S. Fisher, B. I. Halperin, P. A. Lee, and W. F. Brinkman, Phys. Rev. B **25**, 349 (1982).

[3]E. D. Specht, A. Mak, C. Peters, M. Sutton, R. J. Birgeneau, K. L. D'Amico, D. E. Moncton, S. E. Nagler, and P. M. Horn, Z. Phys. B **69**, 347 (1987).

[4]A. D. Novaco and J. P. McTague, Phys. Rev. B **19**, 5299 (1979).

[5]H. Freimuth and H. Wiechert, Surf. Sci. **162**, 432 (1985).

[6]M. Kardar and A. N. Berker, Phys. Rev. Lett. **48**, 1552 (1982).

[7]H. Freimuth, H. Wiechert, and H. J. Lauter, Surf. Sci. **189**, 548 (1987).

[8]J. Cui, S. C. Fain, H. Freimuth, H. Wiechert, H. P. Schildberg, and H. J. Lauter, Phys. Rev. Lett. **60**, 1848 (1988).

[9]H. Freimuth, H. Wiechert, H. P. Schildberg, and H. J. Lauter, Phys. Rev. B **42**, 587 (1976).

[10]S. V. Hering, S. W. Van Sciver, and O. E. Vilches, J. Low-Temp. Phys. **25**, 793 (1976).

[11]D. S. Greywall and P. A. Busch, Phys. Rev. Lett. **65**, 2788 (1990).

[12]D. S. Greywall, Phys. Rev. B **41**, 1842 (1990).

[13]Grafoil is an exfoliated graphite manufactured by Union Carbide.

[14]E. I. Dupont de Nemours, Polymer Products Department, Wilmington, DE, type SP-22.

[15]D. S. Greywall and P. A. Busch, Phys. Rev. Lett. **67**, 3535 (1991).

[16]H. J. Lauter, H. Godfrin, V. L. P. Frank, and H. P. Schildberg, Physica B **165&166**, 597 (1990).

[17]V. L. P. Frank, H. J. Lauter, H. Godfrin, and P. Leiderer, in *Phonon 89,* edited by S. Hunklinger, W. Ludwig, and G. Weiss (World Scientific, Singapore, 1990).

[18]H. J. Lauter, V. L. P. Frank. H. Taub, and P. Leiderer, Physica B **165&166**, 611 (1990).
[19]J. M. Gottlieb and L. W. Bruch, Phys. Rev. B **41**, 7195 (1990).
[20]M. Bretz, Phys. Rev. Lett. **38**, 501 (1977).
[21]M. P. M. de Nijs, J. Phys. A **12**, 1857 (1979).
[22]T. Halpin-Healy and M. Kardar, Phys. Rev. B **34**, 318 (1986).
[23]E. Domany, M. Schick, and J. S. Walker, Phys. Rev. Lett. **38**, 1148 (1977).
[24]M. Bretz, Phys. Lett. **31**, 1447 (1973).
[25]V. Elser, Phys. Rev. Lett. **62**, 2405 (1989).
[26]V. Elser (unpublished).